JOURNAL OF MATERIALS SCIENCE 33 (1998) 4327–4332

Preload relaxation of threaded fasteners in sand-castings of zinc-based alloys

A. A. MIR, S. MURPHY
Aston University, Aston Triangle, Birmingham, B4 7ET, UK

Zinc alloy castings are usually assembled together or mounted by screwed steel fasteners, and are tightened to a predetermined torque to develop the required tensile preload in the fastener. Due to relaxation processes in the castings, creep may cause a partial preload loss at an elevated temperature. The equipment used for load relaxation tests consists of a load-monitoring device, an oil bath, and a data-acquisition system. A load cell monitoring device is used to monitor the load loss in an ISO-metric M6 × 1 steel screw set into sand castings made from alloys No. 3, No. 5 and No. 2 and tightened to produce an initial preload of 6 kN. The castings were held at constant temperature in the range 80–120 °C in an oil bath. The oil bath maintains the desired test temperature throughout the experiment. All tests were conducted for periods of upto 160 h. For all alloys, the initial load loss was high, decreasing gradually with time, but not ceasing. The load loss increased rapidly with test temperature, and almost all of the relaxation curves approximated to a logrithmic decay of load with time. Alloy No. 2 had the best resistance to load loss, with No. 5 next and No. 3 worst at all temperatures. The lower resistance to relaxation of alloy No. 3 was mainly due to the lower relaxation strength of copper-free primary dendrites, whereas in alloys No. 5 and No. 2, the higher copper contents contribute greatly to their relaxation strength in the form of second-phase particles.

1. Introduction

Load relaxation is the time and temperature dependent decrease of load in a material due to conversion of elastic into inelastic (plastic) strain [1]. During this process, the total strain is kept constant, while the load applied initially decreases with time [2]. It has been observed that load relaxation is a problem in rivet and screw joints, particularly in automotive components where the temperature is usually high. It is also considered important in other stressed components, such as wheel rims and consoles for spring brackets in cars that are used in a warm climate [3].

Zinc alloy die castings are widely used for automotive components due to their excellent mechanical properties, near-net shape capability and overall low manufacturing costs. In all these components, fasteners are used to fix them to other components and structures, or join individual parts together. The fasteners (bolts or screws) with normal or self-tapping thread forms are set in pre-threaded or plain holes [4].

A tensile preload in the fastener is produced by tightening the fasteners to a predetermined torque. A small elastic displacement of the clamped parts does not increase the preload of the fastener appreciably, because the fasteners are much less stiff than the bosses or flanges that they clamp together. Therefore, torques may be applied to fastener safely and the initial normal stress is close to the yield stress for the material [5].

It is therefore possible to induce a high preload in the fastener such that the components are joined so tightly together that their relative movement is stopped and the whole structure is integrated for the projected life of the assembly. A study of the stress distributions in steel fasteners set into steel nuts has revealed [6] that most of the loading is concentrated on the first few threads of engagement, and also the distribution of the stress depends critically on the exact dimensions of the threaded parts.

Torque-relaxation has been observed in assemblies subjected to high service temperatures and creep effects may become significant. In automotive applications, the initial preload is lost progressively because vibration may cause gradual rotation of fasteners in their threaded holes. Both effects are detected by an apparent slackening (loss of torque) of the bolt or screw, which may be temporarily rectified by re-tightening. In steel assemblies, this problem has been found to be due to creep elongation of the fastener causing partial loss of the essential preload [7]. Due to the high melting temperature of steel, the creep process in steel fasteners is insignificant at temperatures less than about 350 °C. On the other hand, creep may occur at near-ambient temperatures for zinc-rich alloys [8]. Thus for steel fasteners used in zinc alloy castings at a service temperature of more than 0.4 T_m, where T_m is the melting temperature of zinc alloys, the contribution of fastener creep is negligible, and any

0022–2461

preload relaxation can be attributed to plastic deformation in the casting. During this process, creep allows a gradual displacement of the fastener relative to the casting, so that the preload is reduced.

Although no theoretical studies of this type of creep process are known, recently some preliminary experimental investigations showed [4, 5] that for steel screws in a range of commercial zinc alloy pressure-die castings, preload relaxation occurred rapidly at temperatures below 100 °C.

Since these preliminary tests were undertaken on zinc alloy pressure-die castings at temperatures up to 80 °C, there was therefore a need to investigate the load relaxation process in these zinc alloys at higher temperatures with different casting process, i.e. sand casting. Another objective of this study was to compare the load relaxation behaviour of the commercial zinc alloys under similar testing conditions.

2. Experimental procedure

2.1. The test specimens

The test specimens used for load relaxation tests were made from the sand castings of zinc alloys No. 3, No. 5 and No. 2. Alloys No. 3, No. 5 and pure aluminium were provided by Britannia Alloys and Chemicals Ltd UK in the form of ingots with guaranteed composition, while alloy No. 2 was prepared at the foundry of Aston University.

These high-zinc alloys No. 3, No. 5 and No. 2 represent a series in which the copper content increases from 0 to 0.85 to 2.8%, respectively, whereas aluminium content is constant for all three alloys. The chemical compositions of the alloys were determined, and are listed in Table I. The specimens were of cylindrical shape, having the following dimensions: length, 30 mm; diameter, 13 mm; and bore (threaded), 6 mm.

These specimens for all tests were produced on a lathe in the Manufacturing and Production Engineering Laboratory of Aston University. During the production of the test-pieces, the machining operation was carefully controlled so as to reduce the surface finish variations to a minimum.

2.2. Testing equipment

The equipment used for testing consists of a load-measuring device, an oil bath and a data-acquisition system.

The load-measuring device was used for the continuous monitoring of load in the commercial fasteners used. It consisted of a short tension rod to which the head of the fastener was attached, which reacted the tensile stress in the fastener through a compression load cell. When the casting was screwed onto the fastener, it simulated the effect of inserting a screw into a hole. The load cell was used to measure the force exerted on the screw thread of a casting. It was a small, high capacity load cell, having a range of 0.15–13 600 kg, and its operating temperature range was -54 to 121 °C.

TABLE I Chemical composition of the experimental alloys (wt %)

Alloy	Al	Cu	Mg	Zn
No. 3	4.23	0.008	0.05	Balance
No. 5	3.96	0.84	0.04	Balance
No. 2	4.21	2.79	0.03	Balance

The oil bath was used to heat the specimen and maintain the desired temperature throughout the load relaxation test. The maximum operating temperature of the bath was 150 °C, and the temperature controller attached to the oil bath had a temperature controlling accuracy of $\pm$ 0.1 °C. At one time, up to seven specimens could be placed in the oil bath.

The data-acquisition (logging) system was used to record the results of the tests. The system had a host computer data logging program, linked with a spreadsheet, i.e. Lotus 123. Variable speed logging was another useful feature provided by the program. This allowed one to programme, the data logging speed to suit the application, i.e. at the start of the test, more data readings were recorded than the later stages of the test, and the last time interval between two readings was 1 h.

2.3. Testing procedure

A M6 × 1 (ISO standard) threaded screw was locked into the tension rod, and the load monitor assembled. The test-piece was then threaded onto the screw up to 16 mm depth, which was the desired engagement of the screw. The entire monitoring assembly was dipped into the hot oil at constant required test temperature, and left for about 3 h to stabilize.

To start the experiment, the tension rod and screw were loaded by turning the fine-pitch nut at the top of the rod. This process was continued until an initial load of approximately 6000 N, which was recorded by the load cell, could be achieved. This whole process was completed in a very short time, i.e.15–20 s.

The data-acquisition (logging) system was started as tightening commenced. The preload loss was then continuously monitored by the load cell for a period of up to about 155 h, after which the test was terminated. Up to four tests were carried out simultaneously, and the test temperature was kept constant with a variation of $\pm$ 0.5 °C.

The results of experiments were recorded by the data-acquisition system, and displayed on a computer in the form of time (s) versus load (N) relaxed.

All load relaxation tests were carried out in duplicate, and if results were not satisfactory, i.e. appreciable scatter was found in the results, some additional tests were also performed at those particular test conditions. The average values of the results were calculated and the mean values taken to represent the load relaxation behaviour of these zinc-based alloys.

3. Results and discussion

The retained load (N) was measured continuously and plotted as a function of test time (min.) for all three alloys, and the results are shown in Figs. 1–3. These

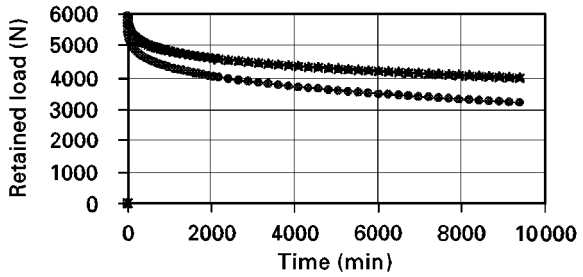

Figure 1 Load relaxation of alloys No. 2, No. 5 and No. 3 at 80 °C –▲– No. 2; –×– No. 5; –●– No. 3.

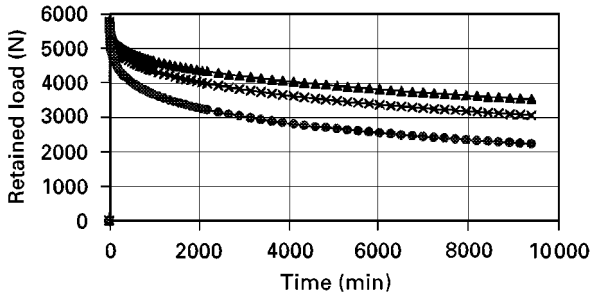

Figure 2 Load relaxation of alloys No. 2, No. 5 and No. 3 at 100 °C –▲– No. 2; –×– No. 5; –●– No. 3.

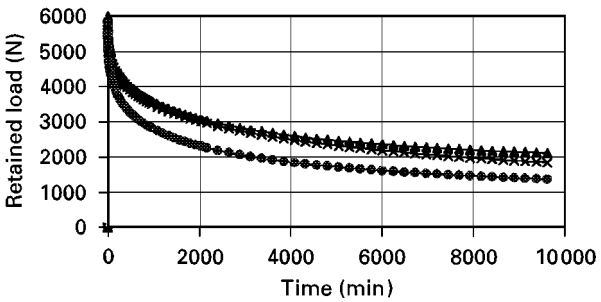

Figure 3 Load relaxation of alloys No. 2, No. 5 and No. 3 at 120 °C –▲– No. 2; –×– No. 5; –●– No. 3.

figures represent the load relaxation data of the experimental alloys obtained for duplicate tests made at 80, 100 and 120 °C, respectively. It was observed that in all cases, the initial load loss was high, decreasing gradually with time, but not ceasing. The amount of load loss increased rapidly with test temperature, and almost all of the curves approximated to a logarithmic decay of load with time, although there was some variation in the initial part of the relaxation curves. This variation was probably due to the effect of localized shear creep of the threads in the castings, which caused a redistribution of the loading.

The results showed clear differences in the comparative resistance to load loss of these alloys. It was revealed that alloy No. 2 had the best resistance to load loss, with alloy No. 5 next and No. 3 worst at all temperatures, as shown in Figs. 1–3. Graphs were drawn to show the variation of retained load (N) with reciprocal temperature at 50, 100 and 150 h for all alloys, as can be seen in Figs. 4–6. From these plots, the effect of short- and long-term load relaxation tests can be observed. The graphs at 50 h time showed the short-term effects of load relaxation, while 150 h time-graphs demonstrated the long-term effect.

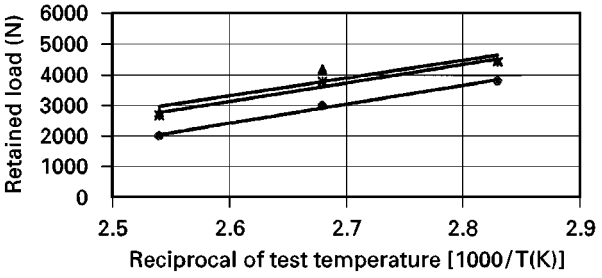

Figure 4 Variation of 50 h load with reciprocal temperature for alloys No. 2, No. 5 and No. 3. ▲ No. 2; ✳ No. 5; ● No. 3.

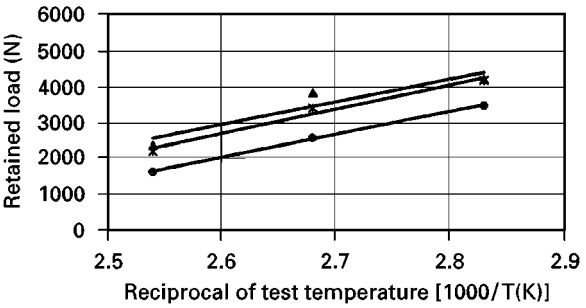

Figure 5 Variation of 100 h load with reciprocal temperature for alloys No. 2, No. 5 and No. 3. ▲ No. 2; ✳ No. 5; ● No. 3.

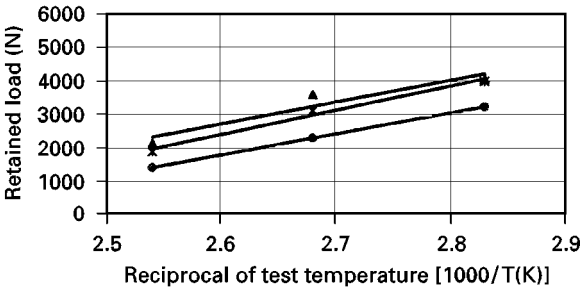

Figure 6 Variation of 150 h load with reciprocal temperature for alloys No. 2, No. 5 and No. 3. ▲ No. 2; ✳ No. 5; ● No. 3.

These plots showed that alloy No. 2 was the best resistant to relaxation, while No. 5 was better than No. 3 at both short and long time periods.

To show the effect of copper content on load relaxation behaviour of alloys, the variation of the retained load (N) against the copper content (%) at different temperatures was plotted at 50, 100 and 150 h, as shown in Figs 7–9, respectively. Alloy No. 3 was much inferior in load relaxation strength than alloys No. 5 and No. 2 at all temperatures; on the other hand alloy No. 2 was better than No. 5, but the difference was greater at 100 °C as compared with other temperatures (Figs 7–9). This indicated that for these alloys, the resistance to load relaxation increased with increasing copper content.

3.1. Microstructural considerations

The structure of the alloys was studied by the scanning electron microscopy (SEM) and optical microscopy. The structure of alloy No. 3 in the as-cast condition is shown in Fig. 10. The figure showed that the structure

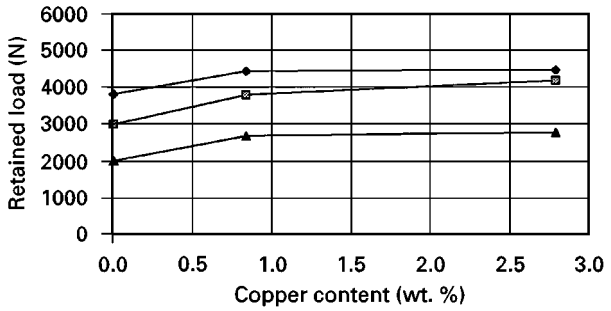

Figure 7 Variation of 50 h load with copper content for alloys No. 2, No. 5 and No. 3. –◆– 80 °C; –■– 100 °C; –▲– 120 °C.

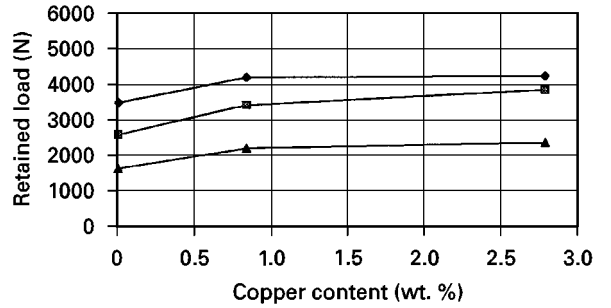

Figure 8 Variation of 100 h load with copper content for alloys No. 2, No. 5 and No. 3. –◆– 80 °C; –■– 100 °C; –▲– 120 °C.

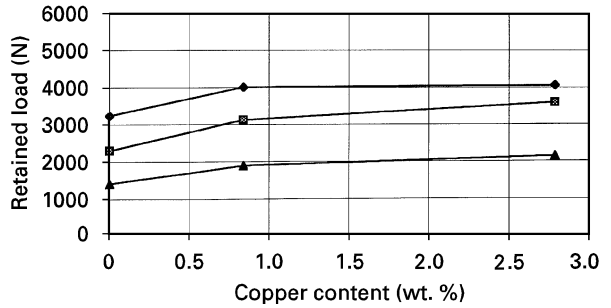

Figure 9 Variation of 150 h load with copper content for alloys No. 2, No. 5 and No. 3. –◆– 80 °C; –■– 100 °C; –▲– 120 °C.

of the alloy was heterogeneous and hypoeutectic, consisting of a few large and numerous small primary zinc-rich (η) dendrites. These primary dendritic particles were surrounded by a relatively small volume of lamellar eutectic (α + η). Many small rounded dark particles of the Al-rich former β phase were attached to the primary η-phase dendrites. These β-phase particles were produced during the eutectic solidification. The β phase is unstable below the eutectoid temperature of about 275 °C and decomposes into Zn-rich η and Al-rich α phases. The edges of the primary η dendrites were also decorated with small and dark Al-rich particles.

The structure of alloy No. 3 after being tested for load-relaxation at 120 °C, is shown in Fig. 11. The scale of the structure was similar to the compressive creep-tested (100 MPa and 160 °C) samples, which can be seen in Fig. 12. The structure consisted of a few large and small primary zinc-rich (η) dendrites surrounded by a lamellar eutectic matrix. Small Al-rich

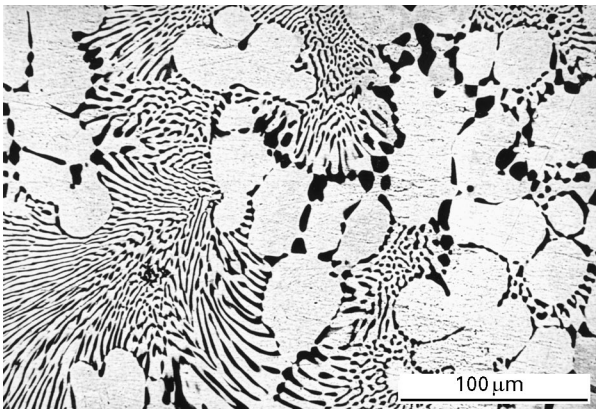

Figure 10 As-cast structure (SEM) of alloy No. 3, showing primary η dendrites and eutectic (α + η).

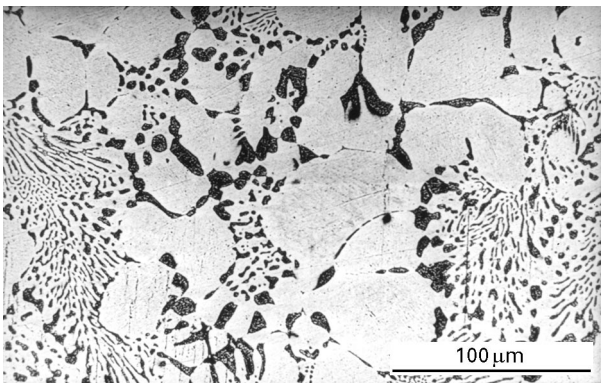

Figure 11 SEM micrograph of the structure of alloy No. 3 tested for load relaxation at 120 °C.

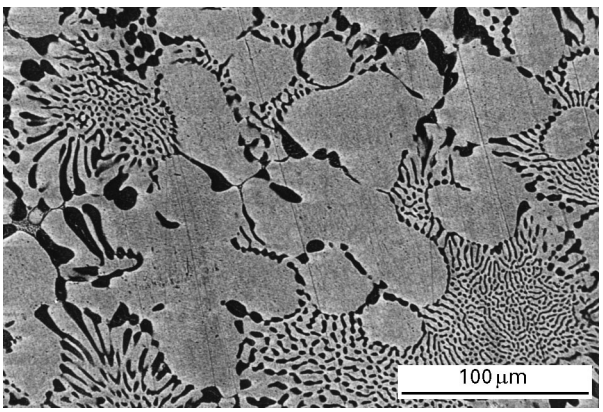

Figure 12 The structure (SEM) of alloy No. 3 tested at 100 MPa and 160 °C.

former β-phase particles were also attached to the primary hypoeutectic η dendrites. The main difference from the structure of the creep-tested sample was that the eutectic matrix lamellae were not as well developed as observed in the creep-tested sample, although they were a combination of short and long lamellar shapes. Generally, these lamellae were smaller than those in the as-cast structure.

Figs 13 and 14 show the structure of alloy No. 5 in the as-cast condition and after load relaxation testing at 120 °C, respectively. The scale of the structure was

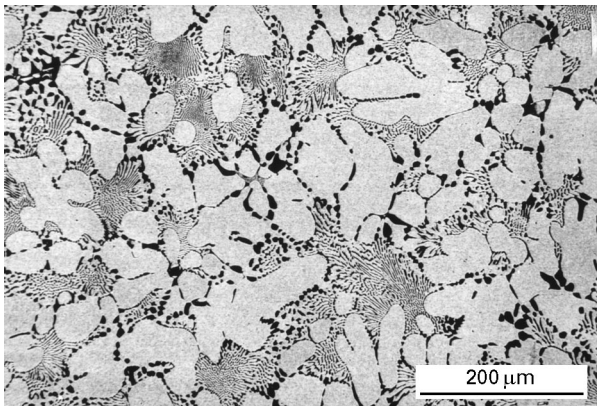

Figure 13 As-cast structure (SEM) of alloy No. 5, showing primary η particles and eutectic.

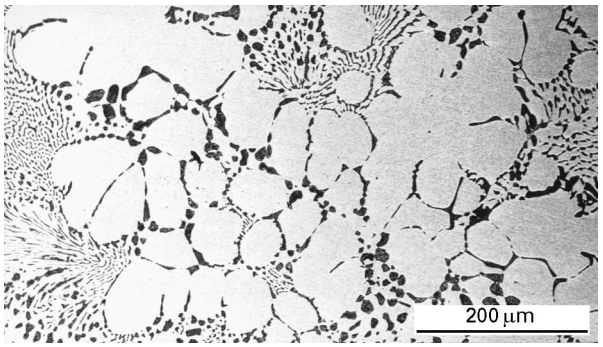

Figure 14 SEM micrograph of the structure of alloy No. 5 tested for load relaxation at 120 °C.

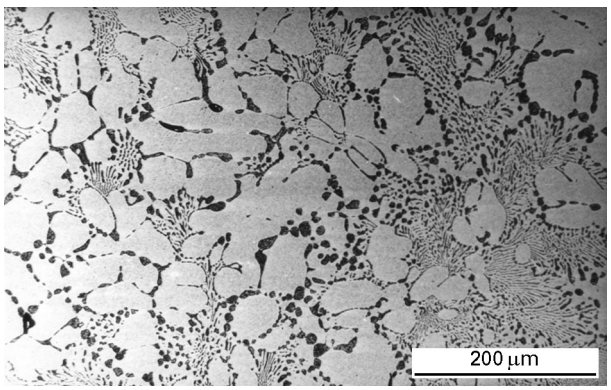

Figure 15 SEM micrograph of alloy No. 5 tested at 20 MPa and 160 °C.

similar to that of alloy No. 3 with more uniformly distributed primary Zn-rich (η) paritcles. Like alloy No. 3, the structure of this alloy also consisted of large and small primary Zn-rich dendrites surrounded by lamellar eutectic (α + η). The main difference from the structure of alloy No. 3 was that the size of primary particles in this case was larger as compared with those of No. 3, also the primary η dendrites and the η component of the eutectic had copper-rich ε-phase precipitates, although it was difficult to differentiate these precipitates from zinc (η) particles due to the very small difference in atomic numbers of both zinc and copper. In the structure of alloy No. 5, the volume of the eutectic matrix was relatively small as compared to primary η particles. Many small and

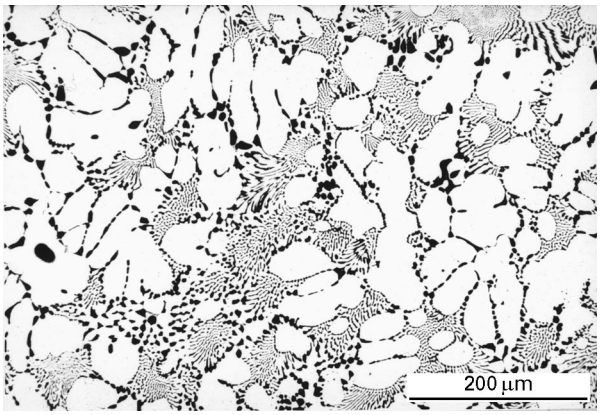

Figure 16 As-cast structure (SEM) of alloy No. 2, showing primary η dendrites and regular lamellar eutectic.

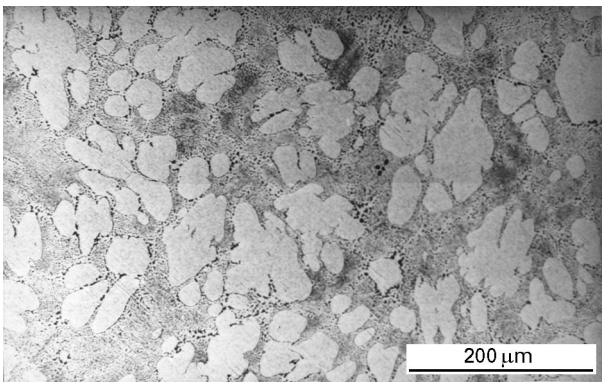

Figure 17 The structure (SEM) of alloy No. 2 tested for load relaxation at 120 °C.

dark particles of Al-rich former β phase were observed, which were attached to the primary η particles, similar to alloy No. 3. β is also unstable below about 275 °C in alloy No. 5, and transforms into Zn-rich η and Al-rich α phases.

The structure of alloy No. 5 after being tested for creep at 20 MPa and 160 °C is shown in Fig. 15. From the micrographs, it was evident that the structures of creep and load relaxation showed close similarities. This similarity of structures indicates that a similar rate-controlling mechanism operates in both types of deformation processes (creep and load relaxation).

The as-cast structure of alloy No. 2 is shown in Fig. 16, whereas Fig. 17 shows the structure of alloy No. 2 after being tested for load relaxation at 120 °C. The structure consisted of large and small primary η dendrites surrounded by an eutectic matrix. The main difference from the as-cast structure was that the eutectic matrix was different. The structure of the sample tested for load relaxation revealed that the eutectic was a mixture of spherodized particles and lamellae, and only a few Al-rich β particles were visible on the edges of primary η dendrites. It was observed that the eutectic structure was coarsened after load relaxation testing. The eutectic and copper particles were more clearly shown in the optical micrograph of alloy No. 2 after testing (Fig. 18).

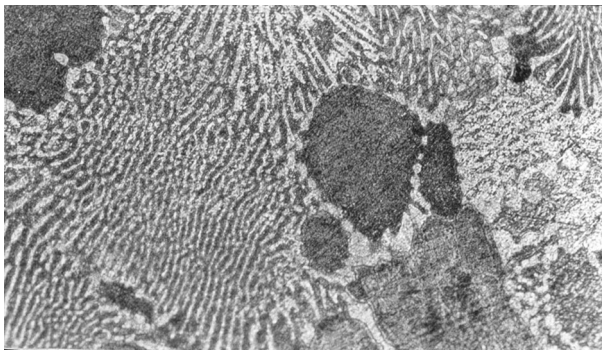

Figure 18 Optical micrograph of alloy No. 2 tested for load relaxation at 120 °C.

3.2. Rate-controlling mechanisms

It is a well known fact that load relaxation is a phenomenon that is closely related to creep and follows the same mechanisms as creep. It is therefore reasonable to analyse the results of load relaxation in the light of general creep theories.

It has already been observed [9] that the rate-controlling mechanism operating in compressive creep of zinc alloys No. 3, No. 5 and No. 2 was dislocation climb. The current load relaxation results may therefore be analysed considering the dislocation climb as a rate-controlling process. From the analysis of load relaxation results and structure of the experimental alloys, it may be concluded that the higher copper content in alloys No. 5 and No. 2 contribute greatly to their relaxation strength in the form of second-phase (ε) particles. These second-phase particles play an important role in preventing dislocation movement, and therefore reducing the relaxation rate as observed for creep experiments on these alloys. The lower resistance to load relaxation of alloy No. 3 was mainly due to the lower relaxation strength of copper-free primary η dendrites, having greater volume than the eutectic in the microstructure (Fig. 10). Copper also influences the precipitation properties of alloys by increasing the precipitate volume and thus gives a certain strengthening. Alloys No. 5 and No. 2 showed much better relaxation strength than alloy No. 3, based on precipitation hardening due to the presence of small copper-rich ε-phase particles. Another well known effect of copper additions to these alloys is a reduced tendency to intercrystalline weakness due to copper-stimulated precipitation within the grains.

4. Conclusions

1. Zinc-rich alloys No. 3, No. 5 and No. 2 showed a rapid initial load loss followed by an approximately logarithmic decay at all test temperatures for times up to 160 h.

2. Alloy No. 2 had the best resistance to load relaxation, with No. 5 next and No. 3 worst at all test temperatures.

3. Alloy No. 2 showed the best resistance to load loss, while alloy No. 5 was inferior to No. 2 but superior to No. 3 for both short- and long-term time periods.

4. The resistance to load loss increased with increasing copper content under all testing conditions.

5. The lower resistance to load relaxation of alloy No. 3 was mainly due to the lower relaxation strength of copper-free primary η dendrites, whereas in alloys No. 5 and No. 2, the higher copper contents contribute greatly to their relaxation strength in the form of second-phase (ε) particles.

6. Dislocation climb was considered as the rate-controlling mechanism for load relaxation in the experimental alloys.

Acknowledgements

The authors would like to thank Dr J.E.T. Penny Head of the Department of Mechanical and Electrical Engineering at Aston University for providing the laboratory facilities for carrying out the experimental work, and Mr Jim Jeffs for his assistance during the tests.

References

1. A. FOX (ed.), Stress Relaxation Testing. ASTM Special Technical Publication 676, Kansas City, MO, 24–25 May 1979 p. 1.
2. F. GAROFALO, in "Fundamentals of Creep and Creep-Rupture in Metals" (MacMillan, New York, 1965) p. 20.
3. J. K. SOLBERG and H. THON, *Mater. Sci. Engng.* **75** (1985) 105.
4. S. MURPHY and F. E. GOODWIN, in International Congress and Exposition, Detroit, MI, 26–29 February 1996, SAE Technical Paper Series (SAE, 1996) p. 1.
5. S. MURPHY and C. W. HAINES, in Proceedings of Advances in Science, Technology and Applications of Zn–Al Alloys, Mexico, 1994, edited by G. T. Villasenor, Y. H. Zhu and C. Pina, p. 3.
6. D. G. SOPWITH, Proc. Inst. Mech. Engng Lond. **159** (1948) p. 373.
7. M. P. MARKOVETS, *Thermal Engng* **17** (1970) 77.
8. "Engineering Properties of Zinc Alloys" (International Lead Zinc Research Organisation Inc., New York, 1989) pp. 41 and 64.
9. A. A. MIR, PhD thesis, The University of Aston in Birmingham (1998).

Received 16 March
and accepted 18 June 1998